Structure prediction, electronic, and mechanical properties of alkali metal MB_{12} (*M*= *Be*, Mg, Ca, Sr) from first principles

Chun-Ying Pu(濮春英), Rong-Mei Yu(于荣梅), Ting Wang(王婷), Zhen-Yan X\"ue(薛振彦), Yong-Sheng Zhu(朱永胜), and Da-Wei Zhou(周大伟)

Citation: Chin. Phys. B, 2021, 30 (**1**): 017102. DOI: 10.1088/1674-1056/abb667
Journal homepage: http://cpb.iphy.ac.cn; http://iopscience.iop.org/cpb

What follows is a list of articles you may be interested in

Electronic structures, magnetic properties, and martensitic transformation in all-d-metal Heusler-like alloys Cd_2MnTM(*TM*=Fe, Ni, Cu)

Yong Li(李勇), Peng Xu(徐鹏), Xiaoming Zhang(张小明), Guodong Liu(刘国栋), Enke Liu(刘恩克), Lingwei Li(李领伟)

Chin. Phys. B, 2020, 29 (**8**): 087101. DOI: 10.1088/1674-1056/ab9739

Structural, electronic, and magnetic properties of quaternary Heusler CrZrCo*Z* compounds: A first-principles study

Xiao-Ping Wei(魏小平), Tie-Yi Cao(曹铁义), Xiao-Wei Sun(孙小伟), Qiang Gao(高强), Peifeng Gao(高配峰), Zhi-Lei Gao(高治磊), Xiao-Ma Tao(陶小马)

Chin. Phys. B, 2020, 29 (**7**): 077105. DOI: 10.1088/1674-1056/ab969b

The role of CALYPSO in the discovery of high-T_c hydrogen-rich superconductors

Wenwen Cui(崔文文), Yinwei Li(李印威)

Chin. Phys. B, 2019, 28 (**10**): 107104. DOI: 10.1088/1674-1056/ab4253

Structural, elastic, and electronic properties of topological semimetal WC-type *MX* family by first-principles calculation

Sami Ullah, Lei Wang(王磊), Jiangxu Li(李江旭), Ronghan Li(李荣汉), Xing-Qiu Chen(陈星秋)

Chin. Phys. B, 2019, 28 (**7**): 077105. DOI: 10.1088/1674-1056/28/7/077105

Prediction of high-mobility two-dimensional electron gas at $KTaO_3$-based heterointerfaces

Fu-Ning Wang(王芙凝), Ji-Chao Li(李吉超), Yi Li(李宜), Xin-Miao Zhang(张鑫淼), Xue-Jin Wang(王学晋), Yu-Fei Chen(陈宇飞), Jian Liu(刘剑), Chun-Lei Wang(王春雷), Ming-Lei Zhao(赵明磊), Liang-Mo Mei(梅良模)

Chin. Phys. B, 2019, 28 (**4**): 047101. DOI: 10.1088/1674-1056/28/4/047101

Structure prediction, electronic, and mechanical properties of alkali metal $M\mathrm{B}_{12}$ (M = Be, Mg, Ca, Sr) from first principles*

Chun-Ying Pu(濮春英)[1], Rong-Mei Yu(于荣梅)[1], Ting Wang(王婷)[2], Zhen-Yan Xüe(薛振彦)[1], Yong-Sheng Zhu(朱永胜)[1], and Da-Wei Zhou(周大伟)[1,†]

[1] College of Physics and Electronic Engineering, Nanyang Normal University, Nanyang 473061, China
[2] Department of Mathematics and Statistics, Nanyang Normal University, Nanyang 473061, China

(Received 30 July 2020; revised manuscript received 27 August 2020; accepted manuscript online 9 September 2020)

Using the particle swarm optimization algorithm on structural search methods, we focus our crystal structures search on boron-rich alkali metal compounds of $M\mathrm{B}_{12}$ (M = Be, Mg, Ca, Sr) with simulation cell sizes of 1–2 formula units (f.u.) at 0 GPa. The structure, electronic, and mechanical properties of $M\mathrm{B}_{12}$ are obtained from the density functional theory using the plane-wave pseudopotential method within the generalized gradient approximations. The formation enthalpies of $M\mathrm{B}_{12}$ regarding to solid metal M and solid alpha-boron suggested the predicted structures can be synthesized except for BeB_{12}. The calculated band structures show $M\mathrm{B}_{12}$ (M = Be, Mg, Ca, Sr) are all indirect semiconductors. All the calculated elastic constants of $M\mathrm{B}_{12}$ satisfy the the mechanical stable conditions. The mechanical parameters (*i.e.*, bulk modulus, shear modulus, and Young's modulus) are derived using the Voigt–Reuss–Hill method. The G/B ratios indicated that the $M\mathrm{B}_{12}$ should exhibit brittle behavior. In addition, the hardness, Debye temperature, universal anisotropic index, and the percentage of anisotropy in compression and shear are also discussed in detail. We hope our results can inspire further experimental study on these boron-rich alkali-metal compounds.

Keywords: first-principles calculations, structure searching, mechanical properties, boron-rich alkali-metal compounds

PACS: 71.15.Mb, 81.40.Jj, 62.20.Dy **DOI:** 10.1088/1674-1056/abb667

1. Introduction

Boron-rich compounds usually exhibit special structure characteristics due to the unique bonding nature of boron. As we all know, boron prefers to bond with five nearest neighbors since it only has three valence electrons, which leads to the existence of the versatile polyhedral frameworks in both elemental B and boron-rich compounds. For example, various boron polyhedral frameworks such as B_4, B_6, and B_{12} clusters were discovered in the boron-rich metal compounds.[1–3] In these compounds, strong covalent bonds are formed between the three-dimensional boron–boron atoms, which can effectively enhance the resistance to plastic deformation, so most metal boron-rich compounds have a high hardness.[4–7] Electronically, the increase of boron content usually opens up a band gap and changes the metal–boron compound to a semiconductor. Among many classes of metal–boron compounds formed by boron clusters, metal dodecaborides ($M\mathrm{B}_{12}$) play important positions. Up to now, a lot of metals such as transition metals lanthanides and actinides were found to form stable dodecaboride phases.[8–10] Due to the existence of B_{12} icosahedra, $M\mathrm{B}_{12}$ usually possess high hardness, high thermal and electrical conductivity, chemical inertness, and superconductivity,[11–18] so they are of great importance in fundamental science and technological applications.

Take the ZrB_{12} as example,[19] which was synthesized and is believed to can be applied in many fields such as hard coatings or anvils of large volume press. More interestingly, most $M\mathrm{B}_{12}$ (M = Zr, Hf, Y, Sc, Tb, Dy, Ho, Er, Tm, Yb, Lu, U, Th, *etc.*) crystalize in unique cubic-UB_{12} (Fm-3m) structure. In this structure, 24 boron atoms form a cuboctahedron cage which contains a metal in its center, and many such structural units are arranged in an fcc lattice.[9] However, ScB_{12} has its own structural type, tetragonal-ScB_{12} ($I4/mmm$),[9] where the cages are arranged in a body centered tetragonal (BCT) lattice. Atomic radii are believed to play a determining role regarding to the different structural types of tetragonal-ScB_{12} and cubic-$M\mathrm{B}_{12}$.[9,19,20] It was revealed that if a transition metal dodecaboride can stably exist under ambient pressure, the metal atoms radius of which must be between those of zirconium ($r_{\mathrm{at}} = 1.55$ Å) and yttrium ($r_{\mathrm{at}} = 1.80$ Å),[9,19] so that the metal atom can fit inside a boron cuboctahedral environment and forms a metal dodecaboride. We noticed that the atom radius of the group-II elements are between 0.89 Å and 1.98 Å, so some of the group-II elements meet the radius conditions and may form stable $M\mathrm{B}_{12}$. At the same time, we found that a lot of $M\mathrm{B}_{12}$ can exist as a metastable state at ambient conditions.

*Projected supported by the National Natural Science Foundation of China (Grant Nos. U1904179, U1904178, and 51501093), the Key Science Fund of Educational Department of Henan Province, China (Grant Nos. 19A140013 and 20B140010), and the Science Technology Innovation Talents Fund in Universities of Henan Province, China (Grant No. 19HASTIT019).

†Corresponding author. E-mail: zhoudawei@nynu.edu.cn

For example, metastable HfB_{12} and ThB_{12} at ambient conditions can be synthesized under high pressure and high temperature conditions,[20,21] so the metastable MB_{12} (M = Be, Mg, Ca, Sr) may also be synthesized at room conditions.

In this paper, we have extensively explored the possible stable phases of MB_{12} (M = Be, Mg, Ca, Sr) at 0 GPa using the particle swarm optimization (PSO) algorithm on crystal structural prediction. We showed the structural diversity of metal dodecaboride, and some of stable semiconducting MB_{12} with new structural type were found. The total energy, lattice parameters, phonon spectra, elastic constants, mechanical parameters, hardness, and the anisotropic factors for the new discovered MB_{12} were investigated systematically using first principles calculations.

2. Computational method

In order to obtain the energetically preferred structures of MB_{12} (M = Be, Mg, Ca, Sr), we used the swarm-intelligence-based structure prediction method as implemented in the CALYPSO code,[22–24] which can effectively search the stable structure for the given compositions. In recent years, the structural prediction method based on the first principles has achieved great breakthrough in the structure prediction of superconductors, superhard materials, and ferromagnetic materials.[25–28] Total energy calculations are performed in the framework of density functional theory within the generalized gradient approximation[30] as implemented in the VASP code.[31,32] The electron–ion interaction is described by pseudopotentials built within the projector augmented wave approximation[33] with s^2p^0, s^2p^0, $p^6s^2d^{0.01}$, $4s^24p^65s^2$, and s^2p^1 treated as valence for Be, Mg, Ca, Sr, and B atoms, respectively. The cut-off energy for the expansion of wavefunctions into plane waves is set to 650 eV in all calculations, and appropriate Monkhorst–Pack k-meshs with grid spacing of $2\pi\times0.03$ Å^{-1} was individually adjusted in reciprocal space with respect to the size of each computational cell. This usually gives total energies well converged within $\sim$ 1 meV/atom. Phonon properties were calculated with the finite displacement method as implemented in Phonopy package[34] with the supercell of $2\times2\times2$ for MB_{12}. In calculating the phonon spectra, the energy convergence criteria were set to 10^{-6} eV for total energy and 0.1 meV/Å for Hellmann–Feynman force.

3. Results and disccusion

3.1. Structures and dynamic stabilities

We firstly performed a test for some MB_{12} (M = Zr, Sc, Lu, U) found experimentally at 0 GPa, the known cubic-UB_{12} (*Fm*-3*m*) and tetragonal-ScB_{12} (*I*4/*mmm*) structures are predicted correctly, which verify the rationality of our predictions. Then we focus our structures search on boron-rich alkali metal compounds of MB_{12} (M = Be, Mg, Ca, Sr) with simulation cell sizes of 1–2 formula units (f.u.) at 0 GPa. The predicted low energy structures of MB_{12} is shown in Fig. 1, the unit-cell parameters and atomic positions of the newly found MB_{12} (M = Be, Mg, Ca, Sr) phases are shown in Table 1. According to our simulations, the structures of BeB_{12} and CaB_{12} stabilize into a tetrogonal structure with space group *I*-4 and *I*-42*m*, respectively. MgB_{12} crystalizes into orthorhombic and SrB_{12} stabilized into cubic, with space group of *Amm*2 and *Pm*-3, respectively. We noticed that all MB_{12} structures show new structural characters, which are different from the previous known structural type of MB_{12} (M = Zr, Sc, Lu, U). In order to describe clearly the difference between the new structures and old ones, we take cubic-UB_{12} (*Fm*-3*m*) as an example. In fact, the typical UB_{12} structure can be considered to be formed in two ways, one is that, take the 24 boron atoms and a metal as a whole unit, and the boron atoms form a cubo-octahedron cage which contains a metal in its center, then many such units are arranged in cubic structure. Another is that, take 12 B atoms and metal atoms as two independent units, respectively, and the 12 boron atoms form a smaller cubo-octahedral B_{12} cluster, while the metal atoms form simple lattices. We tend to descript the newly found stable MB_{12} structures in the latter way. Because that in the predicted structures, the 24 boron atoms do not form a regular cubo-octahedral B_{24} cluster again, while cubo-octahedral B_{12} clusters can still exist. In the newly found MB_{12} (M = Be, Mg, Ca, Sr) structures, the metals form different simple lattices, while the smaller cubo-octahedral B_{12} clusters embeded in the lattices. More interestingly, we notice that the twelve boron atoms in B_{12} cluster are not equivalent and the B–B bonds in the B_{12} cluster are not equal, so the B_{12} cluster in the MB_{12} can be regarded as a distorted B_{12} cluster. We believe that the special structural characterizes found in MB_{12} are attributed to the bond nature of group-II elements, as we have known, the group-II elements only have two valence electrons and do not preferred to bond with so many B atoms, then a regular cubo-octahedral B_{24} cluster does not appear in the MB_{12} structures.

The structural stability is another very important issue, we can estimate the thermodynamics stability of MB_{12} (M = Be, Mg, Ca, and Sr) according to the formation enthalpy simply, *i.e.*, the energy needed to form MB_{12} compounds in those structures. If the formation enthalpy of the MB_{12} is negative, the structures are considered to be energetically favorable and can be prepared by experiment. The formation enthalpies for MB_{12} are calculated by the following equation:

$$\Delta H = E_{\text{Total}}(MB_{12}) - E_{\text{Total}}(M) - E_{\text{Total}}(B_{12}), \qquad (1)$$

where $E_{\text{Total}}(MB_{12})$, $E_{\text{Total}}(M)$, and $E_{\text{Total}}(B_{12})$ are the calculated total energies of MB_{12}, solid M and solid alpha-boron.

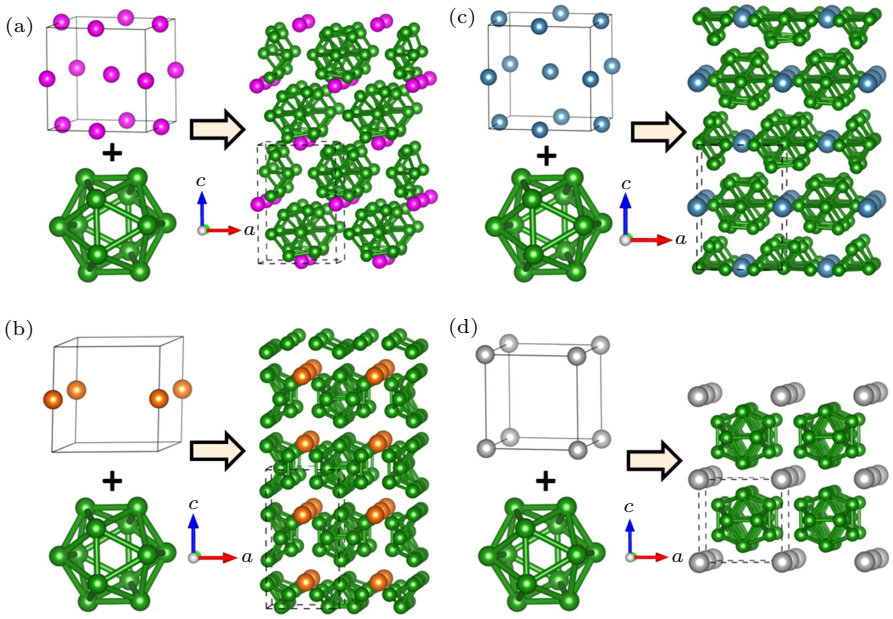

Fig. 1. The crystal structures of (a) BeB_{12}, (b) MgB_{12}, (c) CaB_{12}, and (d) SrB_{12}.

Table 1. The unit-cell parameters and atomic positions of the newly found MB_{12} (M = Be, Mg, Ca, Sr) phases at 0 GPa.

	Space group	Lattice parameters (Å)			Wyckoff positions		
					x	y	z
BeB_{12}	I-4	$a=b=c=5.298$ $\alpha=\beta=122.18$ $\gamma=86.26$	Be	2b	0.0000	0.0000	0.5000
			B1	8g	–0.3318	0.5043	–0.2522
			B2	8g	–0.1960	0.7038	–0.0938
			B3	8g	–0.6265	0.1262	0.0591
MgB_{12}	$Amm2$	$a=4.7882$ $b=4.7778$ $c=9.1120$ $\alpha=\beta=\gamma=90.0$	Mg	2b	0.5000	0.0000	–0.3256
			B1	8f	0.1796	0.1917	–0.4963
			B2	4c	0.3056	0.0000	–0.0905
			B3	4c	0.6895	0.0000	–0.8986
			B4	4d	0.0000	–0.3212	–0.3324
			B5	4d	0.0000	0.3188	–0.6593
CaB_{12}	I-42m	$a=b=c=5.298$ $\alpha=\beta=121.12$ $\gamma=88.07$	Ca	2b	0.0000	0.0000	0.5000
			B1	8f	0.0000	0.3334	0.0000
			B2	16j	–0.3090	0.3089	0.6605
			B3	8i	–0.1378	0.1378	0.8190
SrB_{12}	Pm-3	$a=b=c=4.779$ $\alpha=\beta=\gamma=90.0$	Sr	1a	0.0000	0.0000	0.1664
			B	12k	0.3176	0.1903	0.5000

Table 2. Formation enthalpies of four newly found MB_{12} (M = Be, Mg, Ca, Sr) phases at 0 GPa.

	MB_{12} (eV)	Alpha-B (eV)	M (eV)	ΔH (eV)
BeB_{12}	–83.5886	–80.4638	–3.7647	0.0492
MgB_{12}	–82.8011	–80.4638	–1.5050	–0.0639
CaB_{12}	–84.0873	–80.4638	–1.9289	–0.1303
SrB_{12}	–83.6457	–80.4638	–1.9261	–0.0966

As can be seen from Table 2, the calculated formation enthalpies according to the above formula are 0.05, −0.06, −0.13, and −0.10 eV per unit cell for MB_{12} (M = Be, Mg, Ca, and Sr), respectively. It can be found that except for BeB_{12}, all the predicted compounds can be synthesized via solid M and solid alpha-boron in theory. The formation enthalpy of BeB_{12} is positive, which suggest that it may exist as metastable phase. Interestingly, according to the calculations of formation enthalpies, we noticed that too small radii of M atom is unfavorable to form more stable MB_{12}, and CaB_{12} is considerable to be the most stable structure.

We further to estimate the structural stability according to the phonon dispersion curves, which yield to crucial information about the dynamical properties of the materials. We calculated the phonon dispersion curves and phonon density of states (PHDOS) of the four predicted structures of MB_{12} (M = Be, Mg, Ca, Sr) (see Fig. 2 in details). The absence of imaginary modes in the entire Brillouin zone confirms their dynamical stability. As illustrated in Fig. 2(a), the motion of the B atoms mainly dominated the vabrational states in the low-frequency regimes. However, for MB_{12} (M = Mg, Ca, Sr), due to the lighter mass of B atom, the low-frequency metal atoms (Mg, Ca, and Sr) plays a significant role.

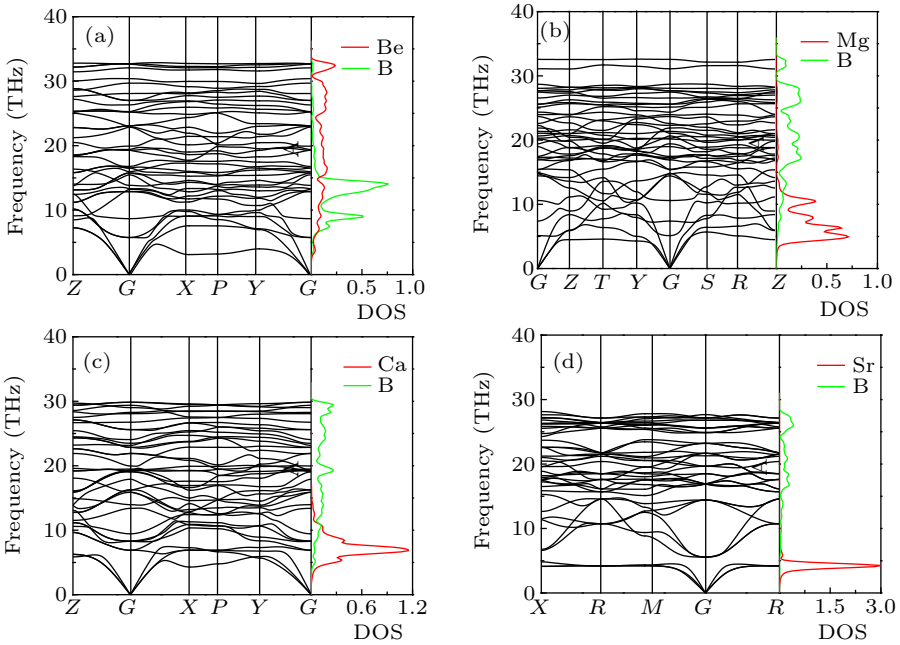

Fig. 2. The phonon dispersion and phonon density of states for (a) BeB_{12}, (b) MgB_{12}, (c) CaB_{12}, and (d) SrB_{12}.

3.2. Electronic properties

To obtain deeper insight into the electronic structures and chemical bonding of these predicted compounds, we calulate the band structures and projected density of states (PDOS) as shown in Fig. 3. We found that all the stable phases of four predicted MB_{12} (M = Be, Mg, Ca, Sr) are indirect semiconductors with band gaps of 0.82, 1.20, 0.03, and 0.92 eV for BeB_{12}, MgB_{12}, CaB_{12}, and SrB_{12}, respectively. To gain deep insight into the electronic structures, we analyzed its total density of states and orbital-projected atomic density of states (see Fig. 3). The valence band maximum (VBM) and the conduction band minimum (CBM) are mainly contributed by the bonding and anti-bonding states of B p orbitals.

We also calculated the electron localization function (ELF) to analyze the bonding features of the structures of MB_{12} (M = Be, Mg, Ca, Sr). Generally, the large ELF values (> 0.5) correspond to the lone electron pairs, core electrons, or covalent bonds, where the ionic bonds are reperesented by small ELF values (< 0.5). An ELF value of 0.5 corresponds with the metallic bond. As shown in Fig. 4, B–B is a covalent bond, which is in agreement with the electronic structures analysis. B–M (M = Be, Mg, Ca, Sr) are the ionic bonds that the electrons are transferred from metal to B atoms, which is further supported by the Bader charge analysis in Table 3.

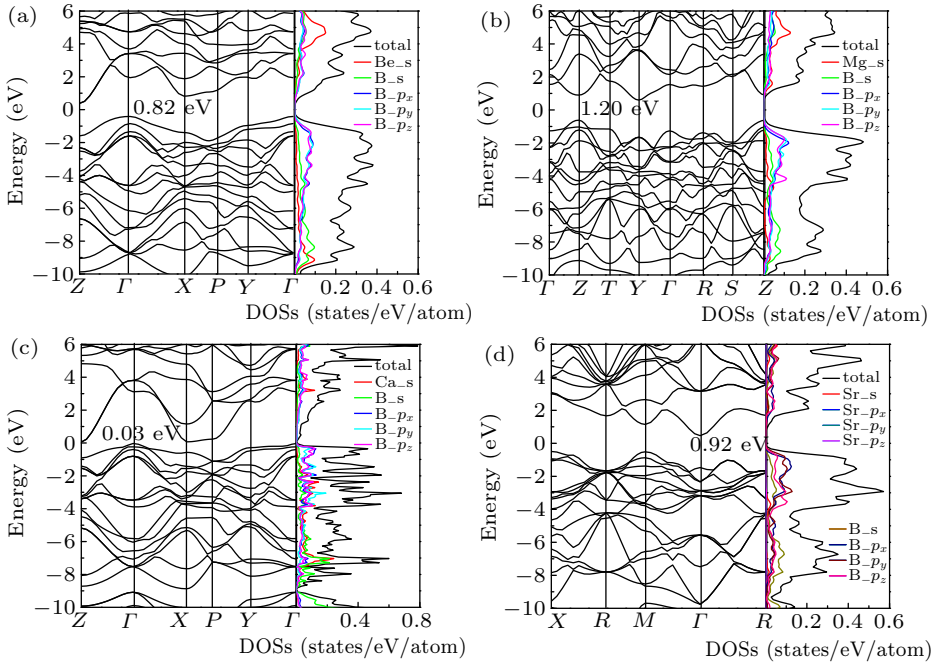

Fig. 3. The band structures and projected density of states for (a) BeB_{12}, (b) MgB_{12}, (c) CaB_{12}, and (d) SrB_{12}.

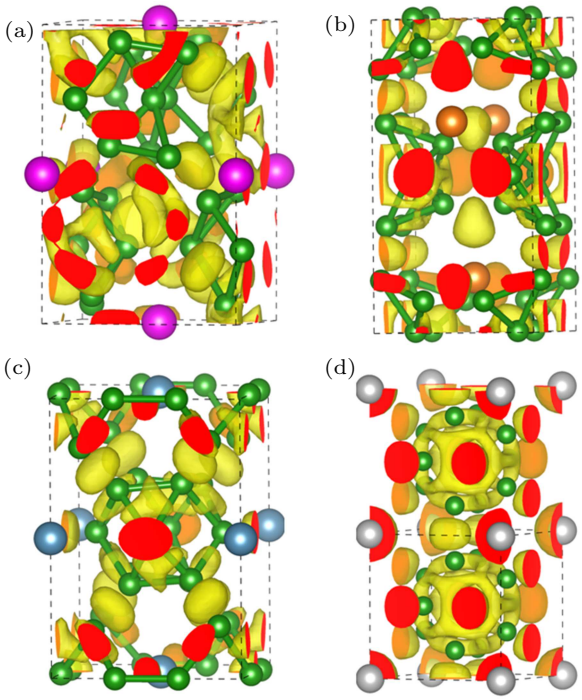

Fig. 4. The electron localization function (ELF = 0.78) of MB_{12} for (a) BeB_{12}, (b) MgB_{12}, (c) CaB_{12}, and (d) SrB_{12}.

Table 4. Bader atomic charge of the predicted structures of MB_{12} (M = Be, Mg, Ca, Sr).

Atoms	Charge	Atoms	Charge	Atoms	Charge	Atoms	Charge
Be	0.33	Mg	0.40	Ca	0.72	Sr	8.56
B_1	3.04	B_1	3.16	B_1	3.09	B_1	3.11
B_2	3.30	B_2	3.20	B_2	3.06	B_2	3.13
B_3	3.05	B_3	3.11	B_3	3.06	B_3	3.02
B_4	3.07	B_4	3.25	B_4	3.09	B_4	3.21
B_5	3.31	B_5	3.32	B_5	3.23	B_5	3.11
B_6	3.06	B_6	3.22	B_6	3.02	B_6	3.22
B_7	3.07	B_7	3.08	B_7	3.23	B_7	3.03
B_8	3.30	B_8	2.96	B_8	3.01	B_8	3.13
B_9	3.04	B_9	3.04	B_9	3.23	B_9	3.10
B_{10}	3.04	B_{10}	3.00	B_{10}	3.01	B_{10}	3.22
B_{11}	3.31	B_{11}	3.07	B_{11}	3.23	B_{11}	3.02
B_{12}	3.06	B_{12}	3.19	B_{12}	3.01	B_{12}	3.13

3.3. Mechanical properties

The elastic constant is essential for many applications related to the mechanical properties of a slid material, epecially for superhard materials. For cubic, tetrogonal and orthorhombic phases, there are four (C_{11}, C_{22}, C_{12}, and C_{44}), six (C_{11}, C_{33}, C_{44}, C_{66}, C_{12}, and C_{13}), and nine (C_{11}, C_{22}, C_{33}, C_{44}, C_{55}, C_{66}, C_{12}, C_{13}, and C_{23}) independent elastic constants, respectively.[35] In terms of the obtained elastic constants, bulk modulus B, shear modulus G, Young's modulus E, and Possion's ratio ν can be evaluated by using the Voigt–Reuss–Hill approximation.[36] The Hill values are defined as the arithmetic average of the Reuss and Voight values

$$B = (B_V + B_R)/2, \quad G = (G_V + G_R)/2, \tag{2}$$

$$E = 9BG/(3B+G), \quad \nu = (3B-2G)/[2(3B+G)]. \tag{3}$$

Cubic phase:[37]

$$B_V = B_R = (C_{11} + 2C_{12})/3,$$

$$G_V = (C_{11} - C_{12} + 3C_{44})/5, \tag{4}$$

$$G_R = 5(C_{11} - C_{12})C_{44}/[4C_{44} + 3(C_{11} - C_{12})]. \tag{5}$$

Tetragonal phase:[38]

$$B_V = (1/9)[2(C_{11} + 2C_{12}) + C_{33} + 4C_{13}], \tag{6}$$

$$G_V = (1/30)(M + 3C_{11} - 3C_{12} + 12C_{44} + 6C_{66}), \tag{7}$$

$$B_R = C^2/M, \tag{8}$$

$$G_R = 15\{(18B_V/C^2) + [6/(C_{11} - C_{12})] + (6/C_{44}) + (3/C_{66})\}^{-1}, \tag{9}$$

$$M = C_{11} + C_{12} + 2C_{33} - 4C_{13} \tag{10}$$

$$C^2 = (C_{11} + C_{12})C_{33} - 2C_{13}^2. \tag{11}$$

Orthorhombic phase:[39]

$$B_V = (1/9)[C_{11} + C_{22} + C_{33} + 2(C_{12} + C_{13} + C_{23})], \tag{12}$$

$$G_V = (1/15)[C_{11} + C_{22} + C_{33} + 3(C_{44} + C_{55} + C_{66}) - (C_{12} + C_{13} + C_{23})], \tag{13}$$

$$B_R = \Delta[C_{11}(C_{22} + C_{33} - 2C_{23}) + C_{22}(C_{33} - 2C_{13}) - 2C_{33}C_{12} + C_{12}(2C_{23} - C_{12}) + C_{13}(2C_{12} - C_{13}) + C_{23}(2C_{13} - C_{23})]^{-1}, \tag{14}$$

$$G_R = 15\{4[C_{11}(C_{22} + C_{33} + C_{23}) + C_{22}(C_{33} + C_{13}) + C_{33}C_{12} - C_{12}(C_{23} + C_{12}) - C_{13}(C_{12} + C_{13}) - C_{23}(C_{13} + C_{23})]/\Delta + 3[(1/C_{44} + (1/C_{55}) + (1/C_{66})]\}^{-1}, \tag{15}$$

$$\Delta = C_{13}(C_{12}C_{23} - C_{13}C_{22}) + C_{23}(C_{12}C_{13} - C_{23}C_{11}) + C_{33}(C_{11}C_{22} - C_{12}^2). \tag{16}$$

The calculated elastic constants were listed in Table 4. From Table 4, it is seen that for these phases, all the elastic constants satisfy the mechanical stable conditions.[40] Although the elastic constants of C_{12} in BeB_{12} is negative, it does not mean an instability because the positive elastic coefficients can be yielded by the actual applied distortions. As we all know, the elastic constants C_{11} and C_{33} characterize the x- and z-direction resistances to linear compression, respectively. We found that C_{11} is higher than C_{33} in both structures of BeB_{12} and CaB_{12}, indicating that the z axis is more compressible than the x axis. For MgB_{12}, the z axis is more incompressible due to the higher C_{33} than C_{11}. Moreover, G/B can be used as mechanical characterization of the compounds. A high (low) G/B value is associated with brittleness (ductility). The critical value, which separates brittle and ductile materials, is about 0.57. The calculated values of the G/B are 0.83, 0.86, 0.89, and 0.93 for BeB_{12}, MgB_{12}, CaB_{12}, and SrB_{12} phases, respectively, and higher than 0.57, which means that the predicted materials would behavior in brittle manner.

Table 4. Calculated values of elastic constant C_{ij} (in unit GPa) and bulk modulus B (GPa), shear modulus G (GPa), the ratio of G and B, Young's modulus E (GPa), Poisson's ratio ν, and the hardness of predicted MB_{12} (M = Be, Mg, Ca, Sr) structures at 0 GPa.

	C_{11}	C_{12}	C_{13}	C_{22}	C_{23}	C_{33}	C_{44}	C_{55}	C_{66}	B	G	E	G/B	ν	H
BeB_{12}	446	–2	140			293	220		127	194	160	376	0.83	0.18	28
MgB_{12}	450	7	54	507	49	462	180	105	104	182	156	364	0.86	0.17	29
CaB_{12}	445	9	122			341	209		151	193	173	399	0.89	0.15	33
SrB_{12}	468	22					127			171	160	465	0.93	0.14	32

On the other hand, the Poisson's ratio ν and Young's modulus E are very important properties for industrial applications. ν provides more information about the characteristics of the bonding forces than any of the other elastic constants. The Poisson's ratio characterizes the stability of the crystal against shearing strain. The low limit and upper limit of ν are given 0.25 and 0.5 for central forces solids, respectively. For a typical metal, the value is supposed to be 0.33; for the ionic-covalent crystal, the value is situated between 0.2 and 0.3; the strong covalent has even small Poisson's ratio, which is usually below 0.15. Calculated ν values are equal to 0.18, 0.17, 0.15, and 0.14 for BeB_{12}, MgB_{12}, CaB_{12}, and SrB_{12} phases, respectively. The calculated Poisson's ratios indicate that the interatomic forces in the MB_{12} (M = Be, Mg, Ca, Sr) are not metal, and there are strong covalent bonding nature in CaB_{12} and SrB_{12}, and they are closed to ionic-covalent crystal for BeB_{12} and MgB_{12}.

On the other hand, the prediction of the hardness of MB_{12} as a superhard material is of great potential interest. We have investigated this aspect further by applying empirical scheme which correlates the Vickers hardness and the Pugh's modulus ratio ($k = G/B$) through the formula $H_v = 2(k^2G)^{0.585} - 3$. According to this equation, the Vickers hardness of BeB_{12}, MgB_{12}, CaB_{12}, and SrB_{12} phases derived from the elastic moduli of Table 3 are estimated to be 28, 29, 33, and 32 GPa, respectively. From Table 3, it has been noticed that four compounds have very small difference of bulk and shear moduli, resulting in the small difference of Vickers hardness between of them, which the hardness values are all lower than that of 40(1) GPa of superhard material ZrB_{12}.[18]

As a fundamental parameter for the materials' thermodynamic properties, the Debye temperature θ_D is related to many physical properties such as elastic constants, specific heat and melting temperature. One of the standard methods to calculate the Debye temperature is from the data of elastic constants, and it may be estimated from the averaged sound velocity v_m by the following equation:

$$\theta_D = \frac{h}{k_B}\sqrt[3]{\frac{3nN_A\rho}{4\pi M}}v_m, \tag{17}$$

where h is Planck's constant, k_B is Boltzmann's constant, n is the number of atoms per formula unit, M is the molecular weight, N_A is Avogadro's number, ρ is the density and v_m is the average sound velocity. In fact, v_m can be obtained from the longitudinal wave velocities v_l and transverse wave velocities v_s

$$\frac{3}{v_m^3} = \frac{1}{v_l^3} + \frac{2}{v_s^3}, \quad v_l = [(B+4/3G)/\rho]^{1/2},$$
$$v_s = (G/\rho)^{1/2}, \tag{18}$$

where B and G are isothermal bulk modulus and shear modulus, respectively. The calculated Debye temperature, average sound velocities, longitudinal wave velocities, and transverse wave velocities are listed in Table 5.

Table 5. Longitudinal (v_l), transverse (v_s), and average sound velocities (v_m), Debye temperature (θ_D), the percentage of anisotropy in compression and shear (A_B and A_G), and universal anisotropic index (A^U) of MB_{12}.

	v_l	v_s	v_m	Θ_θ	A_B	A_G	A^U
BeB_{12}	13386	8394	9243	1387	0	0.086	0.9
MgB_{12}	12610	7983	8782	1306	0	0.056	0.6
CaB_{12}	12601	8048	8844	1309	0	0.036	0.4
SrB_{12}	10765	6943	7621	1116	0	0.037	0.4

For a more comprehensive estimate of MB_{12} elastic anisotropy, we adopt the anisotropy indexes of bulk modulus and shear modulus (A_B and A_G) proposed by Chung and Buessem[41] and the universal elastic anisotropy index A^U developed by Ostoja–Starzewski[42] for crystal with any symmetry. To estimate the anisotropic characteristic of the system, they are

$$A_B = \frac{B_V - B_R}{B_V + B_R}, \quad A_G = \frac{G_V - G_R}{G_V + G_R}, \tag{19}$$
$$A^U = 5\frac{G_V}{G_R} + \frac{B_V}{B_R} - 6 \geq 0, \tag{20}$$

where $A_B = A_G$ =0 represents the elastic isotropic, and $A_B = A_G = 1$ represents the maximum elastic anisotropy. Equation of A^U indicates that the larger deviations from zero imply the higher anisotropic mechanical properties. For isotropy materials $A^U = 0$. Table 5 shows the calculated results of four compounds of MB_{12}. We can see that the anisotropy factor A_B is zero in four compounds, indicating a complete elastic isotropy in compressibility. However, we noted that the value of A_G in BeB_{12} is higher than other three structures, which indicating the larger anisotropy. For A^U, it can be easily seen that CaB_{12} and SrB_{12} have low degree of universal elastic anisotropic behavior due to the smaller A^U.

4. Conclusions

To determine alkali-metal MB_{12} (M = Be, Mg, Ca, and Sr) compounds with their electronic and mechanical properties, we explored the crystal structures and stabilities by using a global-minimum structure prediction, combined with first-principles calculations. We show that the predicted structures are dynamical stable, and pointed out the possible synthesis route via solid M and solid alpha-boron of MB_{12}. From calculated band structure and density of states, the four compounds are all indirect semiconductors. The charge transfer from alkali M to B are responsible for the structural stability. The elastic constants, bulk, shear, and Young's modulus are also predicted. Debye temperature, hardness, and anisotropic factors are also discussed in detail. All the elastic constants satisfy the mechanical stable conditions. The values of G/B suggest alkali-metal MB_{12} materials exhibit as brittleness behavior. The Vickers hardness of four compounds derived from the elastic moduli are estimated to be lower than that of 40 GPa of superhard material ZrB_{12}. The elastic anisotropy was characterized by several different anisotropic indexes ($A_{B,}A_G$, and A^U). Our work provides the basis for further experimental investigations of the alkali-metal MB_{12}.

References

[1] Guo J, Fu H, Zou G, Liu B and Peng Q 2015 *J. Alloys Compd.* **632** 68
[2] Jiang X and Zhao J 2015 *RSC Adv.* **5** 48012
[3] Hermann A, Mcsorley A, Ashcroft N W and Hoffmann R 2012 *J. Am. Chem. Soc.* **134** 18606
[4] Wang M, Li Y W, Cui T, Ma Y M and Zou G T 2008 *Appl. Phys. Lett.* **93** 101905
[5] Liang Y, Gou Y, Xun Y, Zheng Z and Zhang W 2013 *Chem. Phys. Lett.* **580** 48
[6] Gou H, Li Z, Wang L M, Lian J and Wang Y 2012 *Aip Adv.* **2** 012171
[7] Liang Y, Xun Y and Zhang W 2011 *Phys. Rev. B* **83** 220102
[8] Matkovich V I, Economy J, Giese R F and Barrett R 2010 *Acta Crystallogr.* **19** 1056
[9] Placa S L, Binder I and Post B 1961 *J. Inorg. Nucl. Chem.* **18** 113
[10] Akopov G, Sobell Z C, Yeung M T and Kaner R B 2016 *Inorg. Chem.* **55** 12419
[11] Schmechel R and Werheit H 1999 *J. Phys. Condens. Matter* **11** 6803
[12] Werheit H, Filipov V, Shirai K, Dekura H, Shitsevalova N, Schwarz U and Armbrüster M 2011 *J. Phys.: Condens. Matter* **23** 065403
[13] Werheit and Helmut 2009 *J. Phys. Conf.* **176** 012019
[14] Werheit H 2007 *J. Phys. Condens. Matter* **19** 186207
[15] Matthias B T, Geballe T H, Andres K, Corenzwit E, Hull G W and Maita J P 1968 *Science* **159** 530
[16] Mar R W and Stout N D 1972 *J. Chem. Phys.* **57** 5342
[17] Akopov G, Yeung M T, Sobell Z C, Turner C L, Lin C W and Kaner R B 2016 *Chem. Mater.* **28** 6605
[18] Ma T, Li H, Zheng X, Wang S, Wang X, Zhao H, Han S, Liu J, Zhang R, Zhu P, Long Y, Cheng J, Ma Y, Zhao Y, Jin C and Yu X 2017 *Adv. Mater.* **29** 1604003
[19] Slater J C 1964 *J. Chem. Phys.* **41** 3199
[20] Cannon J F and Farnsworth P B 1983 *Journal of the Less Common Metals* **92** 359
[21] Cannon J F, Cannon D M and Hall H T 1977 *Journal of the Less Common Metals* **56** 83
[22] Wang Y, Lv J, Zhu L and Ma Y 2012 *Comput. Phys. Commun.* **183** 2063
[23] Gao B, Gao P, Lu S, Lv J, Wang Y and Ma Y 2019 *Sci. Bull.* **64** 301
[24] Wang Y, Lv J, Zhu L and Ma Y 2010 *Phys. Rev. B* **82** 094116
[25] Xia K, Gao H, Liu C, Yuan J, Sun J, Wang H and Xing D 2018 *Sci. Bull.* **63** 817
[26] Sun Y, Lv J, Liu H and Ma Y 2019 *Phys. Rev. Lett.* **123** 097001
[27] Cui W W, Li Y W 2019 *Chin. Phys. B* **28** 107104
[28] Xu M, Huang C, Li Y, Liu S, Zhong X, Jena P, Kan E and Wang Y 2020 *Phys. Rev. Lett.* **124** 067602
[29] Liu H, Naumov I I, Hoffmann R, Ashcroft N W and Hemley R J 2017 *Proc. Natl. Acad. Sci. USA* **114** 6990
[30] Perdew J P, Burke K and Ernzerhof M 1996 *Phys. Rev. Lett.* **77** 3865
[31] Kresse G and Furthmuller J 1996 *Comput. Mater. Sci.* **6** 15
[32] Kresse G and Furthmuller J 1996 *Phys. Rev. B* **54** 11169
[33] Blöchl P E 1994 *Phys. Rev. B* **50** 17953
[34] Togo A, Oba F and Tanaka I 2008 *Phys. Rev. B* **78** 134106
[35] Wu Z J, Zhao E J, Xiang H P, Hao X F, Liu X J and Meng J 2007 *Phys. Rev. B* **76** 054115
[36] Hill R 1952 *Proc. Phys. Soc. A* **65** 349
[37] Hanies J, Léger J M and Bocquillon G 2001 *Annu. Rev. Mater. Res.* **31** 1
[38] Watt J P and Peselnick L 1980 *J. Appl. Phys.* **51** 1525
[39] Watt J P 1980 *J. Appl. Phys.* **50** 6290
[40] Nye J F 1985 *Physical properties of crystals* (Oxford: Oxford University Press)
[41] Chung D H and Buessem W R 1967 *J. Appl. Phys.* **38** 2010
[42] Ranganathan S I and Ostoja-Starzewski M 2008 *Phys. Rev. Lett.* **101** 055504